Guided Parachutes: A Novel Approach to UAS Safety Over Populated Areas

Mitchell E. Kain[1] and Josiah Z. Walker.[2]
NASA Aeronautical Academy, Langley Research Center, Langley, VA

As the density of autonomous Unmanned Aerial Vehicles increases in local airspaces, the need to ensure they can operate safely over people increases. Traditional parachute solutions for drone failure are inadequate for avoiding populated areas and reducing impact energy. This paper explores the possibility of using guided parachutes as an injury mitigation technology to reduce kinetic energy while simultaneously steering the failed drone away from populated areas to safe landing zones.

I. Nomenclature

C_D	=	Coefficient of Drag
C_L	=	Coefficient of Lift
C_R	=	Coefficient of Lift/Drag Ratio
D	=	Drag force
IMU	=	Inertial Measurement Unit
KE	=	Kinetic Energy
L	=	Lift force
L/D	=	Lift/Drag Ratio
S	=	Surface Area exposed to Windstream
V_T	=	Velocity in the direction of travel
V_H	=	Velocity in Horizontal direction
V_V	=	Velocity in Vertical direction
ρ	=	Ambient air density
φ	=	Glide angle

II. Introduction

To certify unmanned aerial systems (UAS) to fly over population safety standards, technology must be developed to mitigate the risk of harm to people and infrastructure during a system failure. The NASA UAS office has been researching a host of technologies to reduce risk and allow Federal Aviation Administration (FAA) certification of UAS flights over people. Safety provisions are vital for the widespread use of UAS technology. This research aims to mitigate potential harm to people during a UAS failure by reducing kinetic energy to a safe level before it impacts something and reducing the risk of harming vital infrastructure and people.

When deployed, emergency systems need to reduce kinetic energy below a threshold to mitigate damage and injury. The NASA UAS office tasked the team to find a way to reduce the kinetic energy of a 75-pound drone flying at 400 ft down from 30,000 ft-Ib to 58 ft-Ib. The 58 ft-Ib metric was chosen because that is the impact energy level the Range Council Commanders associate with a 50% fatality rate while standing [1]. Parachutes are a common safety solution for UAS flying over populated areas or for those with sensitive payloads. Common commercially available parachutes for UAS in the 75 Ib size and larger often only bring kinetic energy levels down to about 120 ft-Ib or higher and unpredictably drift with the wind [2]. Further research found a few potential solutions, but achieving such high levels of energy reduction will likely require multiple overlapping systems.

[1] Lead Research Associate, NASA Aeronautics Research Directorate. Boston University, MS 2024
[2] Research Associate, NASA Aeronautics Research Directorate. James Madison University, Engineering, BS 2024

In addition to kinetic energy reduction, the ability to steer away from people or sensitive objects is also desirable. In theory, risk could be significantly reduced by simply steering to avoid, decreasing the need to reduce kinetic energy. This steering ability could be paired with a crash management software like SafetoDitch [20]. Autorotation is a technique helicopters use to land during an emergency that allows them to navigate to a safe landing site using fall velocity to spin the propeller and generate lift [8]. Some quadcopters have variable pitch propellers, potentially allowing autorotation, but variable pitch control requires complex swashplates to control the system [3]. Through trade studies accounting for time and resources, it was decided to focus on gliding parachutes, specifically double-keeled para-wing parachutes, also known as Rogallo wing parachutes [4]. These parachutes deploy faster than standard parachutes and can steer to avoid obstacles (if paired with safety software like safe2ditch). They can also steer to mitigate wind drift and act as airfoils generating lift. This lowers the sink rate far below standard parachutes [5]. In addition, the ability to perform a flare maneuver before landing drastically reduces kinetic energy before impact, theoretically exceeding the UAS office target of 58 ft-Ib.

III. Concept Selection

Several trade studies were conducted to ascertain the most direct and effective path to accomplish a kinetic energy reduction to 58 ft-Ib. Factors considered included the maturity of the technology, how effective each type of technology was likely to be based on initial estimations, how familiar the researchers were with the technology, and the time it would take to produce a working model, as this research was conducted over a condensed 10-week period.

A. Considered Technologies

The following is a non-exhaustive list of technologies that were researched for this purpose. They were then rated on feasibility and practicality as well as technology readiness and how well they met the prompt to reduce kinetic energy and protect bystanders.

1. **Airbags**
   A classical method for impact reduction used in everything from car safety systems to Mars landings [6]. Two main subsets exist, explosive deployment that acts to directly push against the impact force and cushioning airbags that deploy to increase the time and surface area of impact.
2. **Auto Pilot Updates**
   Improved, built-in safety precautions, algorithms that see and avoid people and crowded areas while crashing, and more resilient abilities to fly under failure conditions [7].
3. **Auto Rotation**
   Auto Rotation is the primary safety feature present in all helicopters. The pitch of the propellor blades is changed to capture the upward wind as the vehicle falls [8]. The spinning mass of the propellors acts as a flywheel, storing a portion of the vehicle's potential energy as rotational kinetic energy, allowing the vehicle to essentially glide to a lower altitude [8]. Energy stored in the spinning helicopter blades is then converted to arrest its remaining momentum with a flare maneuver [8]. Autorotation has been shown to also work for small drones with collective pitch control [9].
4. **Balloons**
   A rapidly inflatable bladder that would fill with helium from an onboard compressed source. A balloon would arrest a fall by generating a buoyant force.
5. **Crumple Zones**
   Crumple Zones increase the impact duration, reducing the impulse the falling vehicle feels. They provide "cushioning" through non-reusable mechanically deformed zones built into the structure and designed to absorb a certain amount of energy before buckling.
6. **Landing Gear**
   Landing gear would also provide cushioning via non-deformable struts with built-in dashpot and spring dampeners.
7. **Parachutes**
   Parachutes are the most common method of kinetic energy reduction. All parachutes induce drag on an airstream by deploying large-surface-area canopies designed to catch the wind and create a higher-pressure region. Some types of parachutes can be steered and controlled by pulling on different connections. Some can even generate lift, as well as drag and glide.
8. **Toroidal Propellers**

Toroidal propellers are a more recent evolution of propeller blades. They are closed, smooth loops that reduce potential injury from aircraft blades spinning [10]. Although these blades do not reduce the drone's kinetic energy, they are potentially a simple modification to reduce a common source of injury.

B. Researcher Based Limitations

As must be accepted in all research efforts, the team lacked certain skill sets. While competent with basic coding languages such as MATLAB and Python, the team was not in a position to develop new software. Autopilot algorithms, therefore, were given low scores in the trade studies. Additionally, there was a constraint on the time the research project had to develop a solution. While nominally a 10-week project, trade studies were conducted on week 3, leaving 7 weeks for development. This limited technology choices to those that had high technological readiness. As you will see in the charts below, these two primary limitations greatly reduced our pool of technologies to pursue.

C. Concept Effectiveness Trade Study

The first trade study conducted compared all the above concepts and rated their effectiveness and the team's ability to complete the development in the 7-week timeline. Scores were chosen from 0-100% based on how effective the concept was in a category or how confident the team felt skills and time aligned with the given problem. This trade study can be seen below in Table 1. Because the primary impetus of the project was human safety, fall reduction weight was rated to be 85% of concept effectiveness, while 15% of the score was focused on protecting people from injury from rotating propellers. To rank the feasibility of completion in the 7-week period, technical readiness, timeline, and skill were scored. Completion scores were then averaged with the reduction weight to produce a final score. The final score is in the rightmost column of Table 1.

	Effectiveness				Completion			Score	
Method	Fall force reduction	Blade injuries reduction	reduction weight	Effect rank	Tech readiness	timeline	skill	average	
Airbags	50	90	56	6	80	80	85	75.25	3
Auto pilot if single motor failure	85	80	84.25	2	70	60	30	61.0625	6
Autorotation (maple leaf)	75	80	75.75	4	10	5	35	31.4375	10
Autorotation (pitch-controlled rotors)	90	80	88.5	1	80	10	10	47.125	9
Balloons (inflate and float)	80	0	68	5	50	30	50	49.5	8
Crumple zones	35	0	29.75	7	80	80	90	69.9375	5
Guided parachute	90	80	88.5	1	70	80	80	79.625	2
Landing gear	10	0	8.5	9	60	70	60	49.625	7
Parachute	95	0	80.75	3	100	100	100	95.1875	1
Toroidal Propellers	0	90	13.5	8	80	100	90	70.875	4

Table 1. Concept Effectiveness and Feasibility Trade Study.

Based on the results of this study it was discovered that parachutes, guided parachutes, and airbags were the most effective use of the team's time and skills for the 7-week period. These results were then explored more in another independently performed trade study.

D. Systems Effectiveness and Feasibility Trade Study

The most promising individual concepts and concepts were compared to each other in a systems effectiveness and feasibility study shown in Table 2. Concepts were scored according to the team's best knowledge according to the criteria in Table 3 in the appendix. Each criterion was then assigned a weight based on perceived importance.

Impact Energy Reduction concepts		Parachute		Parachute + airbags		Guided parachute + airbags		guided parachute		airbags		auto rotation	
Criteria	weight	Score	weighted score	Score	weighted score	Score	weighted score	Score	weighted score	Score	weighted score	Score	weighted score
Cost	25.00%	4	1	3	0.75	3	0.75	4	1	3	0.75	2	0.5
Human impact energy	25.00%	2	0.5	3	0.75	3	0.75	2	0.5	1	0.25	2	0.5
Time to develop	25.00%	4	1	3	0.75	2	0.5	3	0.75	3	0.75	2	0.5
System Reusability	10.00%	3	0.3	3	0.3	3	0.3	3	0.3	3	0.3	4	0.4
Impact type	15.00%	1	0.15	2	0.3	4	0.6	3	0.45	2	0.3	3	0.45
total score rank total	100.00%	2.95		2.85		2.9		3		2.35		2.35	

Table 2. Systems Effectiveness and Feasibility Trade Study

Based on the results of this study, it was concluded that a parachute or guided parachute would be ideal for our situation. Combined systems were ranked lower because of their increased complexity and time to develop.

E. Trade Study Results

Based on the results of both trade studies, standard parachutes and gliding parachutes were the best options for the given timeline of 7 weeks. If more time and resources were allotted, a combined system of a gliding parachute and airbags may be the most effective way to reduce impact energy. Because another team was implementing a commercial parachute system, it was decided to focus on gliding parachutes. In addition, the team was unable to find commercial solutions that would reduce the impact energy of a drone to less than 58 ft-Ib, but a gliding parachute could theoretically reduce that impact energy to close to zero and steer to avoid sensitive objects [4].

F. Guided Parachute Selection

Several viable options exist for a guided or steerable parachute, including circular, cruciform, ram air, and Rogallo wings [4]. These wings are either shaped to glide (ram air and Rogallo), deformed (cruciform), or have holes strategically cut (circular) to enable forward movement [4].

After significant research, it was determined that the ram air parachute would be the most effective, having the highest lift-to-drag ratio [4]. Unfortunately, it was realized that because of the complexity of making, the lack of viable commercial, and parachute deployment complications, a ram air parachute wasn't feasible for the given timeline [4]. Circular [4] and cruciform parachutes [11] do not have sufficient control authority for effective steering from our goal altitudes, having only a glide ratio of 0.25:1 or 0.50:1, they would only be able to control itself to 100-200 feet from the point it is over. Finally, Rogallo parachutes, used as advanced sky diving reserves, also known as parawings, were explored [4]. Rogallo parachutes are far simpler than ram-air parachutes, having only one layer of fabric [4]. Rogallo parachutes also open faster than most other parachutes, which is ideal for lower-altitude deployments [5]. In addition, a low-cost, commercially available parachute was found to be sold by Apogee Rockets for model rocketry [12]. Because purchasing a parachute and modifying it would help meet the given time constraints and because of the other advantages of the Rogallo parachute, the commercial option was purchased and modified to demonstrate the kinetic energy reduction potential of gliding parachutes.

Even if the timeline allowed for the development of air ram parachutes, the advantages of the Rogallo parachute likely outweigh its comparatively moderately lower glide ratio because of its simplicity and fast deployment rate. Rogallo parachutes are well studied with detailed plans and data in "LOW-SPEED WIND-TUNNEL INVESTIGATION OF ALL-FLEXIBLE TWIN -KEEL TENSION -STRUCTURE PARAWINGS" [13]. The purchased model, named model 5 in the aforementioned paper, has a large range in lift/drag ratio when certain control strings were shortened and had a lot of potential for steering and flaring [13].

IV. Rogallo Parachute Background and Theoretical Feasibility

Using NASA reports on the aerodynamics of Rogallo parachutes and basic drag and lift equations, the theoretical size needed for a 75 Ib UAS is calculated. In addition, the kinetic energy reduction of a parachute and gliding parachute are compared.

The basic drag equation can be rewritten to solve for vertical terminal velocity, V_V, or sink rate, dependent on the weight of the falling object, W, the density of the ambient atmosphere, ρ, the surface area of the falling object, S, and the zero-dimensional drag coefficient, C_D [14]:

$$D = C_D \frac{\rho V^2}{2} S = W \Leftrightarrow V_V = \sqrt{\frac{2W}{\rho S C_D}}$$

Equation 1. Drag Equation and Vertical Velocity Equation

This formula can be used to calculate the sink rate of a falling object at constant speed. If a constant surface area, drag coefficient, and atmospheric density are assumed, the terminal velocity for any weight can be solved to set the baseline for a normal parachute impact-arresting device. Doing the same for gliding parachutes is significantly more complicated because gliding parachutes produce lift and have a forward velocity component. Equation 1 can be manipulated into equation 2 to solve for the velocity of [15]. V_T is the falling object's total velocity, C_L is the lift coefficient, and V_V is the vertical component determined from the glide angle φ, determined from the lift/drag ratio. The V_H can similarly be determined by multiplying V_T by $cos\varphi$.

$$V_T = \sqrt{\frac{2W}{S\rho} \frac{1}{\sqrt{C_L^2 + C_D^2}}} \Rightarrow V_V = \sqrt{\frac{2W}{S\rho} \frac{1}{\sqrt{C_L^2 + C_D^2}}} sin\phi$$

Equation 2. Total and Vertical Velocity of a Gliding Parachute

Now, with an expression for the vertical speed of a theoretical control parachute and a test gliding parachute, the functions can be plotted with weight as the independent variable. The C_L and C_D for a model 5-style gliding Rogallo parachute can be used to calculate the φ from the L/D ratios [13], and circular-style parachutes have a C_D of approximately 1.75 [18]. Equations 1 and 2 can be plotted for V_V on the same axis, showing in Figure 1 that the vertical speed for the gliding parachute is always less than that of the traditional parachute.

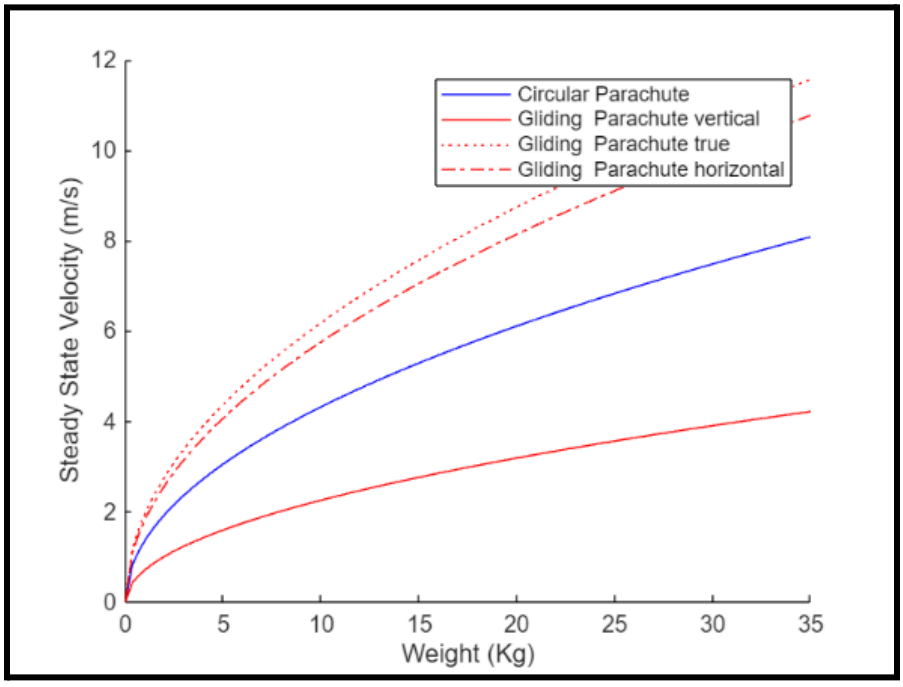

Figure 1. Object mass vs. velocity of a circular and gliding parachute

Reducing velocity reduces the kinetic energy of an object significantly since velocity is squared. This relationship can be seen in equation 3 below, where *KE* is kinetic energy, *m* is mass, and *v* is velocity.

$$KE = \frac{1}{2}mV^2$$

Equation 3. Kinetic Energy Equation

The kinetic energy of a large drone falling from 400ft using a gliding parachute is approximately 313.45 Joules (231.2 ft-lbs.) at 34kg (75lbs approx.). This is still much greater than our goal of less than 58 ft-lbs. However, these equations do not account for a flare maneuver. The difference between the normal ballistic parachute's energy is contained in the horizontal component of the gliding parachute's velocity. This stored kinetic energy can be used to further reduce the impact force. Approximately 1500 ft-lbs. of kinetic energy in the horizontal direction can used for this purpose, and if only 15% of that energy was used to reduce the vertical speed, the total kinetic energy would have reduced impact to less than 58 ft-Ib. There exists a balance point where just enough velocity in both vertical and horizontal axes is built up that a flare maneuver cancels both out completely. This is difficult to calculate and it was decided to experimentally demonstrate this as attempting to model a flexible wing, ground effect, and more would take more time than available.

V. Prototype Design

A subscale prototype was developed to demonstrate a gliding parachute's kinetic and impact energy reduction ability. The commercially available Apogee Rocket Gliding parachute system only uses a single servo for control, so it doesn't have the ability to flare [12]. Flaring requires the ability to pull both control lines down at the same time, so to overcome this limitation, a custom two-servo control system was developed using a Futaba R7008SB receiver, two Tower Pro mg90S, and a 2/3AAA NIMH 4.8V 300mah battery. A diagram of this can be seen in Figure 2.

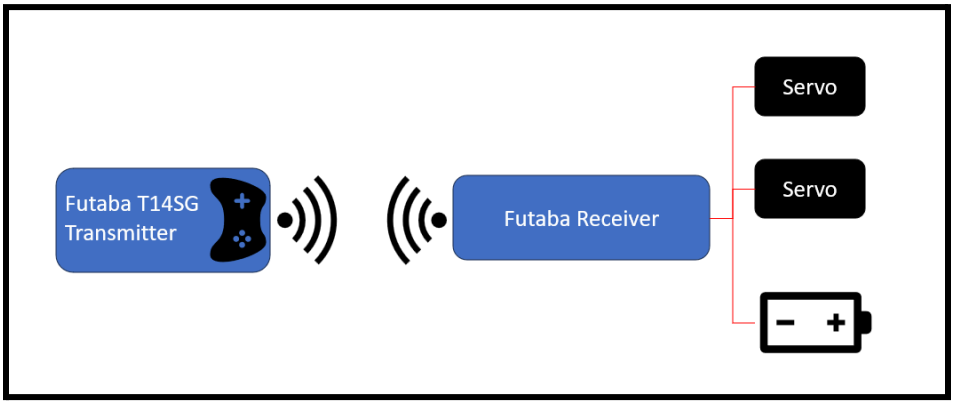

Figure 2: Control System Functional Diagram

The components were encased in a PLA and plywood sandwich structure for modularity and repairability. Control line lengths made from 37-pound kite lines were controlled by the servos through a pully. A PTFE tube was added to prevent the line from getting off track. The structure was designed for easy integration of a TSR Pro Inertial Measurement Unit (IMU) [16], and an ENDAQ IMU [17] was dual lock mounted on the outside. Both of these sensors were selected but only the ENDAQ data was used because the TSR lacked accuracy in the impact energy ranges needed. A Creo model of the control system is shown in Figure 3. The system was wrapped in bubble wrap to protect the system during flight. Pictures of the physical system can be seen in Figure 4.

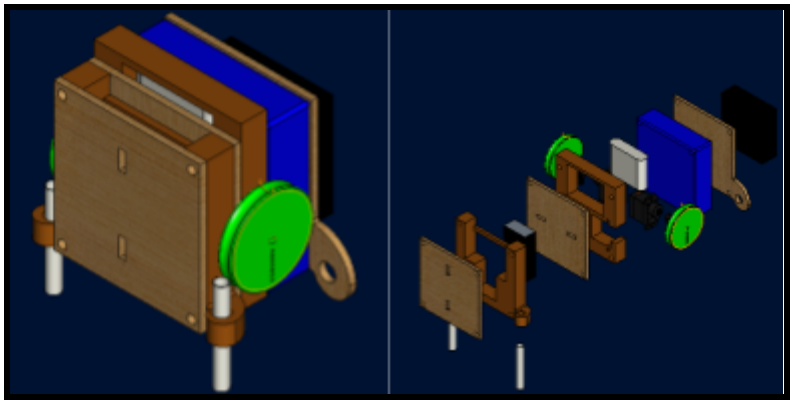

Figure 3. Creo Model of Control Box

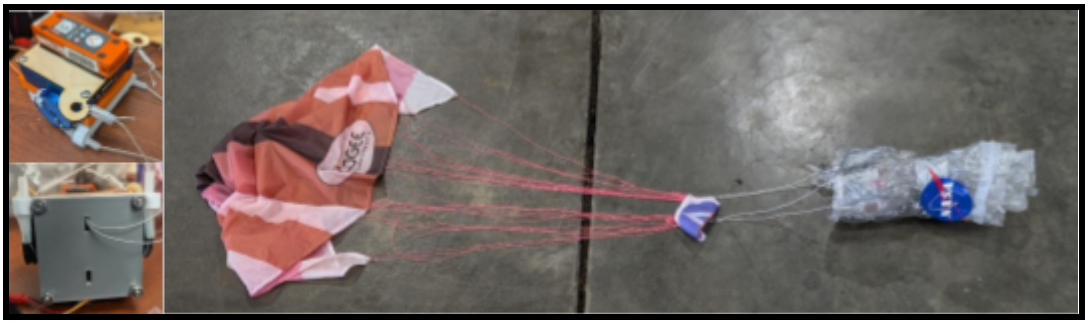

Figure 4. Images of prototype

VI. Sub-scale parachute scaling

Scaling equations validated from experimental testing were used to scale the 3.3Ib subscale gliding parachute from 3.3Ib to 75Ib to demonstrate effectiveness for a 75Ib falling mass. Linhard and Buhler used equation 4, which is based on dynamic scaling methods [21]. This equation will calculate the size needed for a full-scale prototype to achieve similar velocities. W_1 is the full-scale mass, W_0 is the sub-scale mass, S_1 is the full-scale parachute surface area, and S_0 is the sub-scale parachute surface area.

$$\frac{W_1}{W_0} = \left(\frac{S_1}{S_0}\right)^{\frac{3}{2}}$$

Equation 4. Regalo parachute scaling equation [21].

The masses were then entered into equation 4 along with the surface area of the sub-scale prototype parachute surface area, and the value of S_1 was solved in equation 5.

$$\frac{75lbs.}{3.3lbs.} = \left(\frac{S_1}{773.4in^2}\right)^{\frac{3}{2}}$$

Equation 5. Equation 4 with values inserted.

From the calculations described above, S_1 works out to be 6205.6in^2, or about 43ft^2, which works out to a keel length of about 7.5 feet. Ripstop nylon weighs about 2oz per square yard [19], so a 43ft^2 parachute weighs about 9.5oz or just over half a pound, not including the launching mechanism and cordage or considering more advanced materials.

VII. Testing

Acceleration from the onboard ENDAQ IMU was collected during a series of drops to facilitate the verification of theoretical models. This allows the calculation of instantaneous velocity by integrating the time series, allowing the calculation of kinetic energy. This method was chosen as photogrammetry was unavailable at the time, and onboard airspeed sensors would struggle with oscillations because of the parachute. Drift errors common to compounding errors in the use of IMUs are not considered an issue due to the very short duration of the flights, and the integration itself is possible since we know the initial zero velocity point.

Drops were conducted in a controlled hangar environment to remove outside interference, such as cross breezes or updrafts, and to provide a stable testing environment. Additionally, a release device was constructed, essentially a pitchfork made of PVC, to ensure consistent opening of the parachute and releases, as seen in Figure 5.

Figure 5. Deployment tool, "Pitchfork", holding parachute.

Thirteen drops were made from two different heights. Environmental variables such as temperature and pressure were measured by the sensors as well to account for any confounding variables. Drops were initially conducted from 55 feet and then later at 65 feet. The drops were video recorded, when possible, for comparison to data.

VIII. Results

Of the 13 drops conducted, 2 of the best flights were analyzed. An untrained pilot controlled each flight, so only some of the fights had effective flare maneuvers. It also proved difficult to control the test article's flight to maintain a straight flight path. The following is a summary of the useful data collected. All fights produced an acceleration curve like the one shown in Figure 6 for all three directions. The vertical direction or sink rate is of primary concern. The curve for the 4th flight is shown in Figure 6. The difference between the flights is not easily noticeable by inspection and only becomes apparent after the curve is integrated.

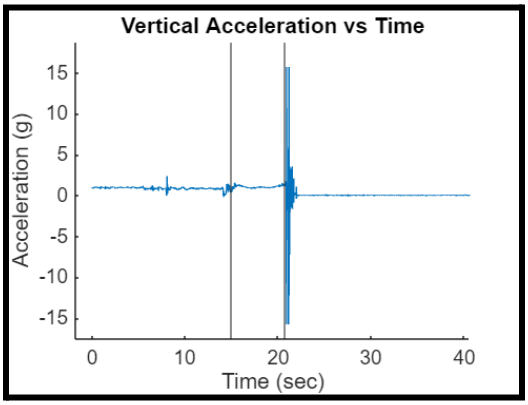

Figure 6. Acceleration curve for the 4th flight

Flight 4 was dropped from 65ft and immediately turned left to avoid drifting too far into the hangar. It dropped, reached a falling velocity of 1.5m/s, then slowed to .75m/s as lift was developed from forward velocity. A flare maneuver was conducted approximately 5ft above ground level, and the vertical velocity was slowed to .5m/s. The flare was conducted too rapidly, and the parachute then stalled and crashed. This flight demonstrated all the goals of

the project: quick deployment, guided/steerable flight, and a successful flare maneuver. The velocity before the flare maneuver was close to the predicted value from our calculations (.75m/s vs .54m/s) this difference is accounted for by the slightly different physical characteristics of our parachute vs the one in the studies our calculations were based on. The graph of this flight can be seen in Figure 7.

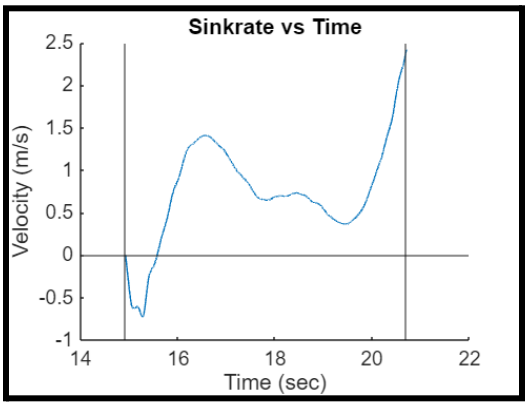

Figure 7. Flight 4 velocity graph

Flight 5 was dropped from 65ft and guided to land at the controller's feet. Its velocity was moderated by the controller to turn and flare for a smooth landing, and the velocity profile is shown in Figure 8. It also reached 1.5 m/s before lift began to develop, then slowed to 0.25 m/s in an early flare before stalling, falling, and hitting the ground.

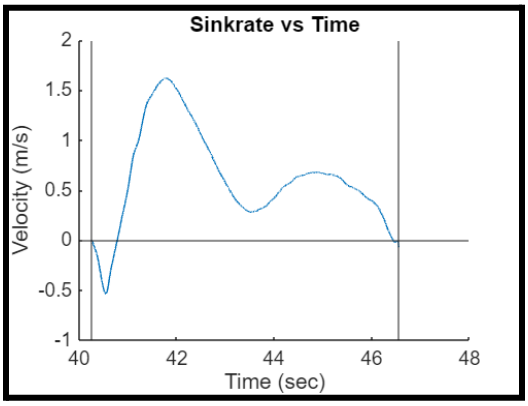

Figure 8. Flight 5 velocity graph

Overall, the results indicate the need for process improvements to eliminate experiment errors, but indicate that our goals are achievable.

IX. Future Work

In the future, the system will be automated with a flight controller to improve the design and results. Automation would monitor sensor data and ensure a straight and consistent attitude flight to reduce errors in post-flight data analysis. Automation would also be able to consistently perform the flare maneuver to remove human error. A controlled flare maneuver could potentially manage the vertical and horizontal kinetic energy such that impact energy is reduced to near zero. In addition, external camera tracking using photogrammetry would improve precision.

Assumptions were made in the data processing steps in order to simplify the physics involved. Angular velocity and acceleration were treated as negligible, and focus was directed entirely at vertical acceleration and velocity. Additionally, the center of mass and the center of lift were all treated as the same point. Future modeling should more accurately account for these factors.

Once this proposed work is completed, this emergency deployment system can be developed, and a full-scale deployable version can be added to a drone for testing. A landing zone selection algorithm can be developed (similar to safte2ditch [20]) to select a location for landing away from populated areas. Additionally, a wheeled landing gear system could be added to account for any unintentional lateral velocity on landing.

Acknowledgments

The authors thank Liz Ward, Matt Coldsnow, Matt Underwood, and Gary Qualls for their help with this project.

References

[1] Westat Inc Rockville Md, "Range Safety Criteria for Unmanned Air Vehicles Rationale and Methodology Supplement" Defense Technical Information Center, Fort Belvoir, VA, April 2001. https://doi.org/10.21236/ADA385238

[2] "Parachute Descent Rate Calculator | Fruity Chutes." Retrieved 7 August 2024. https://fruitychutes.com/help_for_parachutes/parachute-descent-rate-calculator

[3] "Variable-Pitch Quadrotor - Aerospace Controls Laboratory." Retrieved 7 August 2024. https://acl.mit.edu/projects/variable-pitch-quadrotor

[4] T. Knacke, "Steerable Parachutes," Defense Technical Information Center, Sep. 1969. https://apps.dtic.mil/sti/pdfs/AD0905223.pdf.

[5] "Peak of Flight Newsletter : Apogee Rockets, Model Rocketry Excitement Starts Here." Retrieved 7 August 2024. https://www.apogeerockets.com/Peak-of-Flight/Newsletter585

[6] "Opportunity - NASA Science." Retrieved 6 August 2024. https://science.nasa.gov/mission/mer-opportunity/

[7] Sun, S., Cioffi, G., De Visser, C., and Scaramuzza, D., "Autonomous Quadrotor Flight Despite Rotor Failure With Onboard Vision Sensors: Frames vs. Events," *IEEE Robotics and Automation Letters*, Vol. 6, No. 2, 2021, pp. 580–587. https://doi.org/10.1109/LRA.2020.3048875

[8] "Autorotation | SKYbrary Aviation Safety." Retrieved 7 August 2024. https://skybrary.aero/articles/autorotation

[9] FliteTest, "Flite Test - Stingray 500 - OVERVIEW," YouTube, Dec. 02, 2013. https://www.youtube.com/watch?v=TnGhEInTXYc (accessed Jan. 16, 2025).

[10] "Toroidal Propeller | MIT Lincoln Laboratory," www.ll.mit.edu, 2022. https://www.ll.mit.edu/partner-us/available-technologies/toroidal-propeller-0

[11] S. M. Herrington, J. T. Renzelman, T. D. Fields, and O. A. Yakimenko, "Vertical Wind-Tunnel Testing of Steerable Cruciform Parachute System," Journal of Aircraft, vol. 56, no. 2, pp. 747–757, Mar. 2019, doi: https://doi.org/10.2514/1.c035106.

[12] "32"GlidingParachuteSystem."Retrieved 8 August 2024. https://www.apogeerockets.com/Building-Supplies/Parachutes/Gliding-Parachutes/32in-Gliding-Parachute-System

[13] Fournier, P. G., "Low-Speed Wind-Tunnel Investigation of All-Flexible Twin-Keel Tension-Structure Parawings."

[14] "Velocity During Recovery." Retrieved 8 August 2024. https://www.grc.nasa.gov/www/k-12/VirtualAero/BottleRocket/airplane/rktvrecv.html

[15] Knacke, T. W., "Parachute Recovery Systems Design Manual."

[16] "TSR PRO & TSR PRO-HB | Diversified Technical Systems," Dec 15 2017. Retrieved 8 August 2024. https://dtsweb.com/tsr-pro-tsr-pro-hb-2/

[17] "S3 Vibration Sensor (S3-D16) | enDAQ | enDAQ." Retrieved 8 August 2024. https://endaq.com/collections/endaq-shock-recorders-vibration-data-logger-sensors/products/s3-vibration-sensor-s3-d16

[18] NASA, "Velocity During Recovery," NASA Glenn Research Center, https://www.grc.nasa.gov/www/k-12/VirtualAero/BottleRocket/airplane/rktvrecv.html (accessed Aug. 24, 2024).

[19] "Ripstop Nylon Fabrics | Seattle Fabrics." Retrieved July 2024. https://www.seattlefabrics.com/Ripstop_c_75.html

[20] L. Glaab et al., "Safe2Ditch Autonomous Crash Management System for Small Unmanned Aerial Systems: Concept Definition and Flight Test Results," National Aeronautics and Space Administration, Nov. 2018. Accessed: Jan. 17, 2025. [Online]. Available: https://www.researchgate.net/publication/346926255_Safe2Ditch_Autonomous_Crash_Management_System_for_Small_Unmanned_Aerial_Systems_Concept_Definition_and_Flight_Test_Results

[21] E. Linhart and W. Buhler, “Wind Tunnel and Free Flight Investigation of All-Flexible Parawings at Small Scale,” National Aeronautics and Space Administration , Jun. 1969. Accessed: Jan. 17, 2025. [Online]. Available: https://www.2e5.com/kite/nasa/reports/19700010491_1970010491.pdf

Appendix I: Trade studies

Criteria #1: Cost	
Score	Can we afford it?
1	likely not
2	potentially
3	Probably
4	Definitely
Criteria #2: Human Impact energy	
Score	Impact energy
1	>128 ft-ib
2	58-128 ft-ib
3	25-58 ft-ib
4	<25 ft-ib
Criteria #3: Time to develop	
Score	acheivable in 7 weeks?
1	likely not
2	potentially
3	Probably
4	Definitely
Criteria #4: System Reusability	
Score	Scale (mi)
1	Irreparible damage
2	Repairable
3	reusable but slow/hard
4	Easily reusable
Criteria #5: Human impact type	
Score	Scale (mi)
1	Hard
2	soft
3	avoidance + hard
4	avoid + soft

Table 3. Systems Effectiveness and Feasibility Trade Study Scoring Criteria